IEEE Access
Multidisciplinary | Rapid Review | Open Access Journal

Received May 11, 2018, accepted May 29, 2018, date of publication June 4, 2018, date of current version June 29, 2018.

Digital Object Identifier 10.1109/ACCESS.2018.2843261

Improved Dark Channel Prior for Image Defogging Using RGB and YCbCr Color Space

ZAHID TUFAIL[1], KHAWAR KHURSHID[2], AHMAD SALMAN[2], IMRAN FAREED NIZAMI[2], KHURRAM KHURSHID[1], AND BYEUNGWOO JEON[3], (Senior Member, IEEE)

[1]Department of Electrical Engineering, Institute of Space Technology, Islamabad 44000, Pakistan
[2]School of Electrical Engineering and Computer Science, National University of Sciences and Technology, Islamabad 44000, Pakistan
[3]Sungkyunkwan University, Suwon, South Korea

Corresponding author: Khawar Khurshid (khawar.khurshid@seecs.edu.pk)

ABSTRACT Environmental factors such as fog and haze affect the image quality and make it unsuitable for automated systems, such as intelligent vehicles, surveillance, and outdoor object recognition, which require images with clear visibility for processing and decision making. In general, reconstruction of fog-free image from a single input image is quite challenging. Dark channel prior (DCP) method is used to estimate atmospheric light for the purpose of image defogging. This paper presents a DCP-based image defogging method with improved transmission map to avoid blocking artifacts. The transmission maps are computed for RGB and YCbCr color spaces. Three transmission maps for the R, G, and B channels are utilized to compute a mean transmission map. In the YCbCr color space, Y channel is used to calculate the transmission map. The two transmission maps are refined by preserving edge information for constructing two intermediate images, which are assigned different weights to get the enhanced defogged output. The proposed method is evaluated against the current state-of-the-art approaches, and the experimental results based on structural similarity index, fog effect, anisotropic quality index and degradation score are calculated, which show that the defogged images reconstructed using the proposed method achieved better results with lower fog effect, similarity index, degradation score and higher quality index value. Reconstructed image has better contrast and luminance which is perceptually more appealing to the human visual system.

INDEX TERMS Dark channel prior, image defogging, image reconstruction, transmission map, image enhancement.

I. INTRODUCTION

The perceptual quality of outdoor scene images is important for understanding and analyzing the environment to perform automated tasks such as navigation, object detection and recognition. Scattering or absorption of light in adverse weather due to fog and haze can greatly restrict the visibility of outdoor scenes. Therefore, images taken in such weather conditions suffer from lower contrast, faded colors and luminance imbalance, resulting in objects far from camera almost invisible. Fig. 1. illustrates the effect of fog which diminishes the visibility in acquired images. It can be seen that image degradation in such condition is due to the reflection and absorption of light by the fog particles. Since reduced visibility greatly effects the imaging systems, automated methods to enhance visibility in foggy images have become an area of interest for researchers. The fog effect depends on the depth of the object in a scene, i.e., the objects farther from the camera lose more information. The models used to reconstruct enhanced images are categorized into two types, physical and non-physical models [1]. Physical model is designed for observing physical causes that degrade the image and based on this model an inverse process is proposed to reduce the degradation level [7]–[9]. Non-physical models are based on image processing techniques that enhance the image contrast and color reconstruction without taking into consideration the factors which caused degradation [1].

Physical models offer the advantage of making local repair according to mist concentration in local regions of the image and offer good defogging results, as proposed in [2]. Tan [3] divided the outdoor images taken in clear weather, into small patches and calculated lowest intensities for each patch. The resultant channel is termed as the Dark Channel, which is used as prior information to reconstruct fog free images [1], [3], [4], [9]–[13]. A dark channel prior (DCP) based method consists of four steps, i.e., atmospheric light estimation, transmission map calculation,

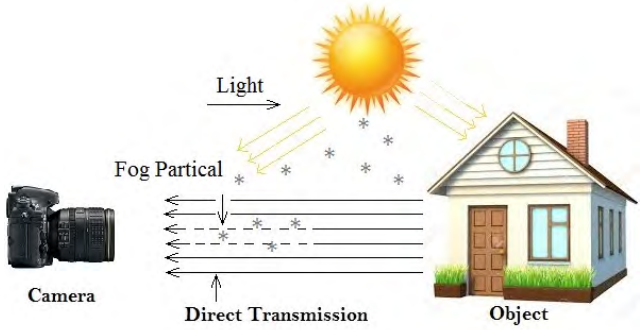

FIGURE 1. Image degradation phenomenon in the presence of fog particles.

refinement of transmission map and reconstruction of fog free image. The dark channel is used to estimate the atmospheric light, the transmission map is the effect of fog on the object which depends on the distance between object and the camera, the transmission map is refined as discussed in section 3, and the last step is the construction of fog free image. DCP is effective for defogging based on the observation that foggy images produce relatively higher intensities in the dark channel as compared to the clear images [4]. He *et al.* [1] observed that the DCP based methods produce result with low brightness, therefore, they proposed to increase the brightness of input image first and then estimate atmospheric light. They applied morphological operations to calculate fog density. Kumari *et al.* [5] applied morphological operations on the grayscale foggy image and then refined by utilizing guided filter for correct estimation of the atmospheric light. DCP method is applied to find the transmission map without any preprocessing or post processing, which results in low intensity and halo artifacts in the defogged image. In [6], quad-tree decomposition and entropy-based weighted contextual regularization is proposed and the brightest region of DCP is used to estimate atmospheric light. Moreover, statistical properties of input image are used to compute boundary constraints adaptively with a quad-tree decomposition to divide foggy image into homogeneous patches. Meng *et al.* [7] proposed a method in which boundary constraints are applied on transmission map combined with contextual regularization based on weighted norm. The geometric perspective of DCP is utilized by applying boundary constraints in which each pixel affected by fog is considered as part of atmospheric light estimated from dark channel prior (DCP). Brightest pixel from each channel of foggy image is selected, and the fog free image is estimated by linear extrapolation of atmospheric light and foggy image. Eight Kirsch operators and a Laplacian operator are used for improving edges and corners. Riaz *et al.* [8] observed that the patch size used for the calculation of dark channel had a major effect on DCP based method. They proposed an edge preserving method with large window size and performed patch-wise maximum operation after applying minimum operator to reduce haloes in the output image. In [9], it was observed that DCP based method is not valid for images containing bright regions without adjusting the transmission map. For such images, atmospheric light is estimated using two different methods. For example, in images with significant sky region, they calculated the histogram of dark channel and set a range of gray levels which correspond to the sky region, and from this range the most frequent gray values are used to estimate the value of atmospheric light. DCP is then applied to estimate the atmospheric light for the non-sky region. Fixed tolerance threshold parameters K and α, along with the transmission map are used to segment out sky region from the image. In [10], a parameter K is proposed to distinguish the sky from the rest of the image. The transmission map for sky is calculated separately, in addition to the original transmission map for non-sky area. It is observed that the low brightness in output image is due to smaller values of the transmission map, hence the parameter 'p' ranging between 0.08 to 0.25 is added in the transmission map. Deng *et al.* [11], proposed a method based on Fuzzy Logic Controller (FLC) that automatically estimates a threshold parameter to overcome the problem of bright region. Chen and Sun [12] used an energy veil to implement a guided filter. The energy veil is obtained by selecting the minimum intensity value from the RGB channels of the foggy image. The energy veil is then used to compute the illumination veil which is the combination of atmospheric light and the transmission map. Yao *et al.* [13] proposed a method based on depth information of the neighboring pixels to reduce edge halation. They observed that edge intensity in fog-free image is always higher and the pixels present at one side of edge have different depth field with respect to pixel present at the other side of that edge. Atmospheric light is estimated in two steps, first Gaussian blur is applied on the foggy image, then RGB space image is converted into YIQ space (Y represents luminance, I represents in-phase, Q represents quadrature), and Y is referred to as atmospheric light. Edge information is obtained by applying Sobel operator, and valid edges are differentiated from noise using a threshold value. Abbaspour *et al.* [14], employed a three step method based on the theory of Koschmieder for atmospheric vision. Morphological operators are applied to find the fog density at different regions in the image. First a low pass filter is applied to estimate the reference intensity, then logarithmic operator is used to estimate target intensity model. A nonlinear transmission operation based on exponential function is applied to reconstruct the foggy region of image. The atmospheric veil is obtained using the exponential behavior of atmospheric veil and the DCP. Tarel and Hautiere [15] observed that two major effects of fog on the images are image contrast and brightness. They reported that image contrast is reduced due to exponential property of intrinsic luminance that reduces the object visibility. Therefore, white balancing is performed before applying defogging. They applied two constraints on physical properties of image which assume that the atmospheric veil is always positive and it cannot be greater than minimum intensity of the foggy image. Yoon *et al.* [16] proposed a defogging algorithm by applying DCP on YCbCr color space. The transmission map is obtained from the regions with

high frequency content and the smooth regions are ignored. In [17], a tone mapping method based on image gradient to defog images is proposed where the edge information is obtained from foggy image for the estimation of transmission map. A gradient based tone mapping algorithm is applied to defog the image. It is observed that the atmospheric light is not estimated correctly by DCP based methods, therefore depth information is obtained from edge detail to estimate atmospheric light. Furthermore, the transmission map is refined using soft matting operation to reduce edge halation. According to He *et al.* [18] the computation of transmission map is the most difficult step of the defogging algorithm. There are three types of prior information i.e. global prior, local prior and similarity prior that are mostly used to compute the transmission map using two assumptions i.e., the minimum value of scene radiance is 0 and depends on the neighboring pixels whereas, the depth of all the pixel in one patch is same and transmission map is consistent within the patch. Lee *et al.* [19] studied four main steps of DCP in detail and compared different defogging methods based on estimation of atmospheric light, calculation of transmission map, refinement of transmission map and reconstruction of image. They proposed that the Gaussian filter and bilateral filters do not require any guidance signal, whereas the soft matting process, cross-bilateral filter and guided filter require a guidance signal to refine transmission map. Tang *et al.* [20] proposed binary tree method to estimate atmospheric light. They set a parameter to divide image into two parts dark region and the bright region, and separately calculated transmissivity for both parts. Then they refined both the transmissivity by applying guided filter. Anwar and Khosla [21] proposed DCP based algorithm with the combination of Weighted Least Square and High Dynamic Range methods. They first removed fog from image by applying DCP based method and then applied WLS based smoothing filter to preserve the edge information. Then they applied HDR based tone mapping to enhance color contrast of reconstructed image. Pal *et al.* [22] proposed a pixel based non-local approach to dehaze image. They estimated transmission map and true image scene for each pixel. Reconstructed image contrast was not good and image looks unnatural, so they applied S-shaped tone mapping based on modified histogram to enhance image contrast. Li and Li [23] proposed DCP based method and observed that refinement of transmission map needs improvement. They performed white balance to estimate air light correctly and propose an improved bilateral filer to refine transmission map. Zhu *et al.* [24] observed that in DCP based method, transmission map is not correctly estimated, and unwanted artifacts in reconstructed image can be removed by improving the transmission map. They estimated transmission map by applying energy minimization and applied piecewise smoothing filter to refine transmission map. Chengtao *et al.* [25] observed that outdoor foggy image usually consists of two distinguished parts i.e. sky portion and the non-sky portion and pixels intensities of both the regions are completely different from each other. They observed that reconstruction of fog free image without comprehensive consideration of sky region results in low brightness in restored image. They segmented out sky region from image and proposed an improved dark channel prior method for both the regions using an adaptive factor. They separately estimated atmospheric light and transmission map for both the regions and reconstructed two fog free images. The final fog free image is obtained by fusing two images and the noise is removed by applying guided filter. Jackson [26] proposed in bright channel technique with combination of dark channel. Bright channel is an inverse of dark channel and it is obtained by selecting maximum intensity values from small patch of each color channel. They selected 0.1% pixels with highest intensity from both the channels and calculated mean value as atmospheric light. They calculated another atmospheric light, by selecting highest intensity value from pixel location of dark channel and bright channel, to estimate transmission map and refined transmission map by applying fast guided filter. Li and Zheng [27] observed that the image reconstructed from DCP based method usually has bad color contrast when transmission map is not correctly estimated or refined. To preserve the fine gradients, they proposed globally guided image filter (G-GIF). The filter is constructed by combining global structure transfer filter and global edge-preserving smoothing filter. Nair and Sankaran [28] proposed an image defogging method using image with three color spaces RGB, Lab and HSV. Each channel of RGB image is processed separately and from Lab and HSV images, intensity channel is used to calculate transmission map. The transmission map is then refined by applying center surround filter and fog free image is reconstructed. Color channels of Lab and HSV color spaces are processed to overcome color distortion in restored image. Although the above mentioned techniques proposed improvements in image defogging in several ways, one or the other method still suffer from issues such as haze effect present in the image after defogging, artifacts introduced by defogging methods, and lack of color contrast in the image. This paper presents an image defogging method based on DCP with an improved transmission map. Three transmission maps based on RGB channels and one transmission map based on the Y channel of YCbCr color map are computed. The mean of three transmission maps obtained from RGB color space is obtained which is termed as the mean transmission map. The mean transmission map and the transmission map obtained from YCrCb color map are refined by preserving the edge information. Two images are reconstructed using the transmission maps. Each image is assigned a weight and fused to reconstruct a final fog free image. The experimental results show that the proposed method produces better results as compared to state-of-the-art image defogging techniques. The major contributions of the proposed method are as follows,

1. An improved and refined DCP through edge preservation is implemented.
2. Correctly estimation of atmospheric light from dark channel using larger patch size.

3. Transmission maps based on RGB and YCbCr have been employed for the reconstruction of fog free images.
4. The proposed method enhances the quality of foggy images and reconstructs images with better structural detail and improved color range.

The rest of the paper is organized as follows, DCP is discussed in section 2, proposed methodology is presented in section 3, and Section 4 presents the experimental results followed by conclusion in section 5.

II. DARK CHANNEL PRIOR

In 1975, McCartney designed a model to represent the degradation mechanism due to fog in images. This model is used in reverse order in most of the physical methods to estimate fog free image in foggy conditions and is given as,

$$I(x) = J(x)\,t(x) + (1 - t(x))\,A \tag{1}$$

where $I(x)$ represents the observed foggy image, A represents the global atmospheric light, $J(x)$ represents the fog-free image and t(x) represents the transmission map. Transmission map is given as,

$$t(x) = e^{-\beta d(x)} \tag{2}$$

Where β is the fog factor and $d(x)$ represents depth in the image. For the image taken in clear weather, $\beta \approx 0$ and its effect is neglected and we get $I \approx J$. On the other hand, when image is taken in foggy weather then $\beta > 0$ and it becomes non-negligible. In (1) $J(x)t(x)$ is the direct attenuation and $A(1 - t(x))$ is the atmospheric light. The image is divided into small patches of size Ω. A minimum filter is applied on local patches of the three RGB channels. Image obtained by using this process is dark with low intensity values. Atmospheric light and transmission map are required to reconstruct the fog free image. Atmospheric light is estimated from the Dark channel. Dark channel of an image I is calculated as:

$$I_{Dark} = \min_{C\in\{R,G,B\}} \left(\min_{y\in\Omega(x)} \left(I^C \right) \right) \tag{3}$$

where I^C represents the intensity values of individual channels of image I, c is the color channel of RGB and I_{Dark} is the dark channel. For the image captured in clear weather, most of the pixels in the dark channel have intensity values close to zero as shown in Fig. 2. When image is captured in foggy weather then number of pixel with high intensity values in the dark channel become significantly large which is the main reason to use dark channel as prior information and atmospheric light is estimated from dark channel.

The transmission map is derived from (1) by normalizing with atmospheric light A and then applying minimum filter on local patches of the image as derived in (4) and (5),

$$\min_{y\in\Omega(x)} \left(\frac{I(x)}{A} \right) = t(x) \min_{y\in\Omega(x)} \frac{J(x)}{A} + 1 - t(x) \tag{4}$$

$$\min_{C\in\{R,G,B\}} \left(\min_{y\in\Omega(x)} \left(\frac{I^C(x)}{A^C} \right) \right) = t(x) \min_{C\in\{R,G,B\}} \left(\min_{y\in\Omega(x)} \left(\frac{J^C(x)}{A^C} \right) \right) + 1 - t(x) \tag{5}$$

From the DCP we know that the following term in (5) is negligible,

$$\min_{C\in\{R,G,B\}} \left(\min_{y\in\Omega(x)} \left(\frac{J^C(x)}{A^C} \right) \right) \approx 0 \tag{6}$$

therefore $t(x)$, the transmission map is given as,

$$t(x) = 1 - \min_{C\in\{R,G,B\}} \left(\min_{y\in\Omega(x)} \left(\frac{I^C(x)}{A^C} \right) \right) \tag{7}$$

Images reconstructed from this transmission map look unnatural and artificially painted. Therefore, parameter ω in the range between [0, 1] is used to make the defogged image natural. The value of ω is adjusted to control the fog factor.

$$t(x) = 1 - \omega \min_{C\in\{R,G,B\}} \left(\min_{y\in\Omega(x)} \left(\frac{I^C(x)}{A^C} \right) \right) \tag{8}$$

The above equation shows the previously proposed transmission map calculation process in the literature. After estimating A and calculating transmission map $t(x)$, fog free image is reconstructed as,

$$J(x) = \frac{I - A}{t(x)} + A \tag{9}$$

III. PROPOSED METHODOLOGY

A. IMPROVED DARK CHANNEL PRIOR

An improved Dark Channel Prior (DCP) based method to reconstruct fog free images is proposed in this work. Fig. 3. shows the block diagram of proposed method. DCP is calculated for two different color spaces, i.e., RGB and YCbCr. A window size of 31 × 31 is used to apply the minimum filter on the RGB images to obtain DCP. First, the minimum filter is applied on the three color channels and then on the local patch of the output image from the filtered RGB image. A large patch size is used for this purpose because smaller patch may yield an erroneous estimation of the atmospheric light. DCP for the RGB color space is given as,

$$I_{Dark} = \min_{y\in\Omega(x)} \left(\min_{C\in\{R,G,B\}} \left(I^C \right) \right) \tag{10}$$

In our case, $\Omega = 31$ for the local patch size. The proposed method also uses DCP on the Y channel of YCbCr color space, which is given as,

$$I_{Dark-Y} = \min_{y\in\Omega(x)} (I_Y) \tag{11}$$

where I_Y is the Y channel of the foggy input image and $\Omega = 31$ is local patch size.

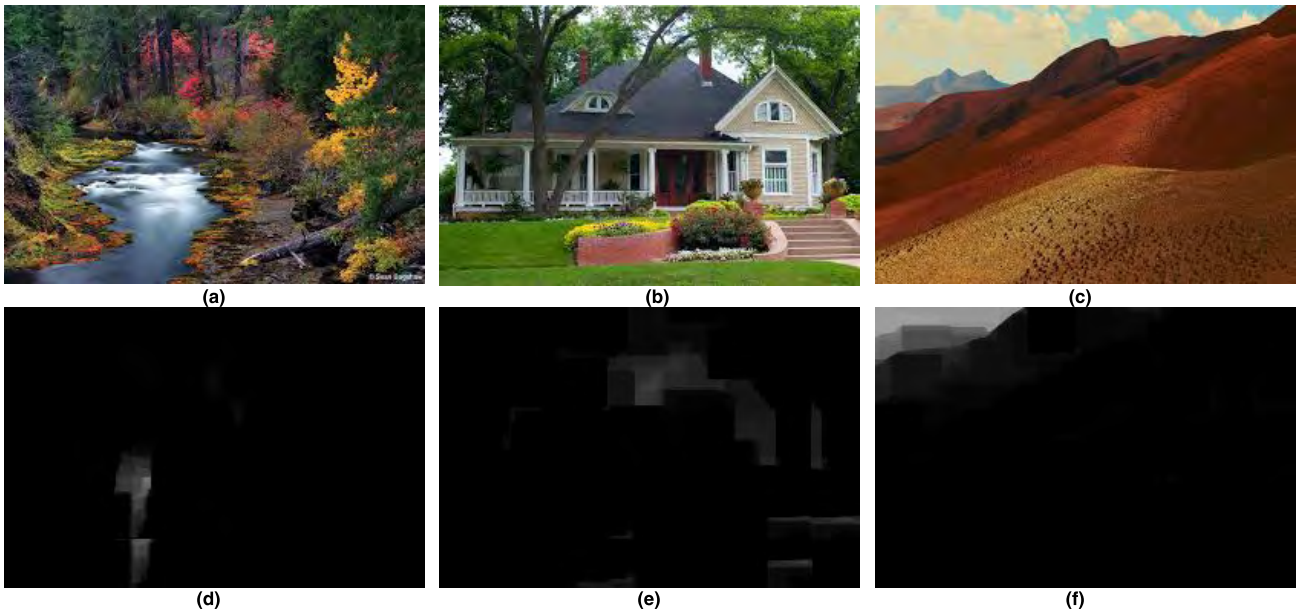

FIGURE 2. Input images in clear weather [(a), (b), (c)] and the corresponding dark channels [(d), (e), (f)].

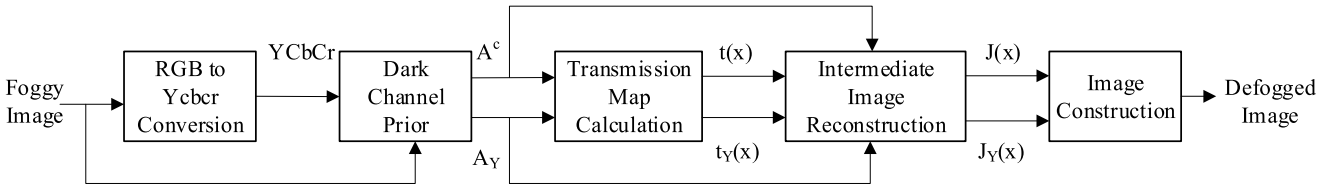

FIGURE 3. Block diagram of the proposed method.

B. ATMOSPHERIC LIGHT ESTIMATION

After computing the DCP from RGB and YCbCr color spaces, the atmospheric light A and A_Y are estimated from dark channels I_{Dark} and I_{Dark-Y}, respectively. The coordinates of the brightest 0.1% pixels are selected and the highest intensity value in each RGB color channels is obtained separately from these pixel locations. These three intensity values from the RGB channels are taken as atmospheric light A, hence A is a 3x1 vector where each value represents the highest intensity value in the individual R, G, and B channel. The same process is also repeated for I_{Dark-Y} to obtain A_Y. The 0.1% brightest pixels that are used to estimate A and A_Y are represented by red pixels in the images shown in Fig.4 (c) and (d) along with their dark channels (a) and (b).

C. TRANSMISSION MAP CALCULATION

The transmission map is computed using the atmospheric light A from the input image. Every channel of input image is divided by its corresponding value in A to compute three transmission channels. The mean channel for RGB color space is computed as

$$t'(x) = 1 - \omega \frac{1}{3}\left(\sum_{C=1}^{3}\left(\frac{I^C}{A^C}\right)\right) \tag{12}$$

In the next step $t'_Y(x)$ is computed as

$$t'_Y(x) = 1 - \omega\left(\frac{I_Y}{\max(A_Y)}\right) \tag{13}$$

where $t'_Y(x)$ is transmission map using channel Y.

D. REFINEMENT OF TRANSMISSION MAP

The transmission map is refined by preserving the information of the gradients. First, Laplacian filter is applied on the transmission map, and the output gradients are subtracted from the original transmission map to remove the unwanted noise. Afterwards, a mean filter is applied for smoothing. The aforementioned process is applied to both the transmission maps i.e., the mean transmission map for the RGB color space and the transmission map for the Y channel of YCbCr color space. The refined transmission maps are shown in Fig.5(a) and (b), which provide significant improvement over the previous approach.

E. RECONSTRUCTION OF FOG FREE IMAGE

After computing all the parameters, the final step is to reconstruct the enhanced image with minimized fog effect.

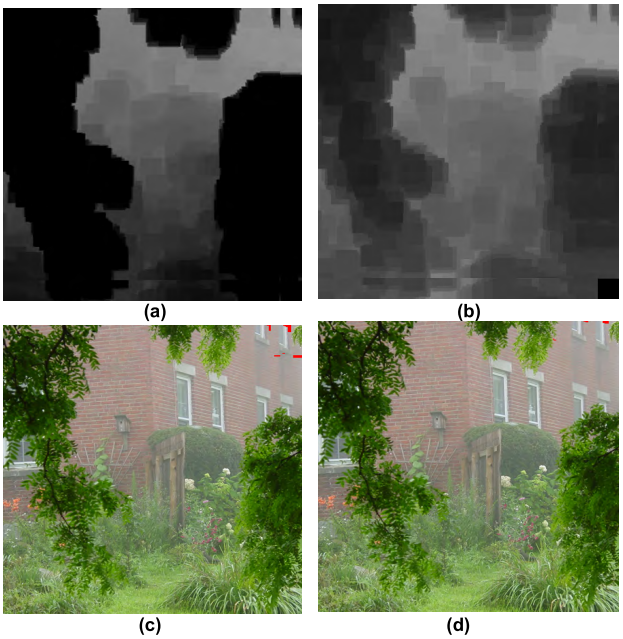

FIGURE 4. (a) Dark channel calculated by (10), (b) Dark channel calculate by (11), (c) Indication of air light calculated by I_{Dark} with red pixels, (d) Indication of air light calculated by I_{Dark-Y} with red pixels.

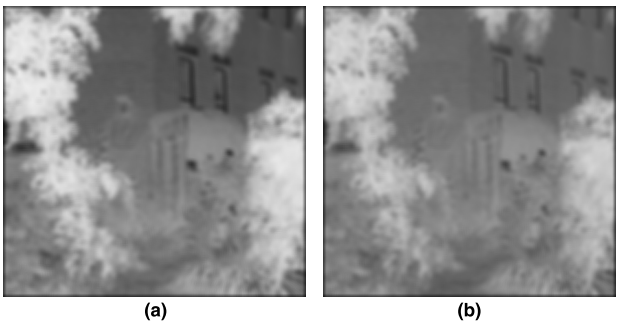

FIGURE 5. (a) Refined transmission map by (12), (b) Refined transmission map by (13).

The image reconstruction process is given by,

$$J(x) = \frac{I - A}{\max(t(x), t_0)} + A \tag{14}$$

$$J_Y(x) = \frac{I - A_Y}{\max(t_Y(x), t_0)} + A_Y \tag{15}$$

Where t_0 is a constant used to avoid division by very small value. $J(x)$ is the image reconstructed using the RGB color space and $J_Y(x)$ is the image reconstructed using the YCrCb color space. Image reconstructed using (14) is darker in shade as shown in Fig.6 (b) and (d) while the image reconstructed using (15) is comparatively lighter as shown in Fig.6(a) and (c). These two images are combined to reconstruct fog-free image. A parameter α is used as a weight to combine these images.

$$R(x) = \alpha J(x) + (1 - \alpha) J_Y(x) \tag{16}$$

where $R(x)$ is the final reconstructed image. The value of α is set as 0.5. Final reconstructed images along with the foggy input images are shown in Fig.7(b), (d) and (f).

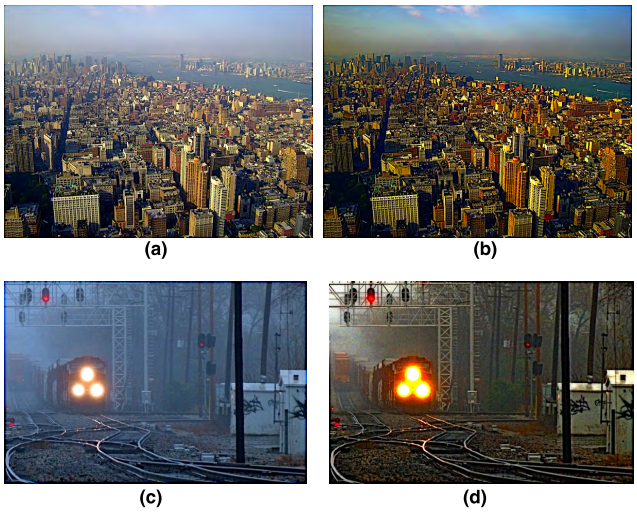

FIGURE 6. (a)(c) Image reconstructed by (15), (b)(d) Image reconstructed by (14).

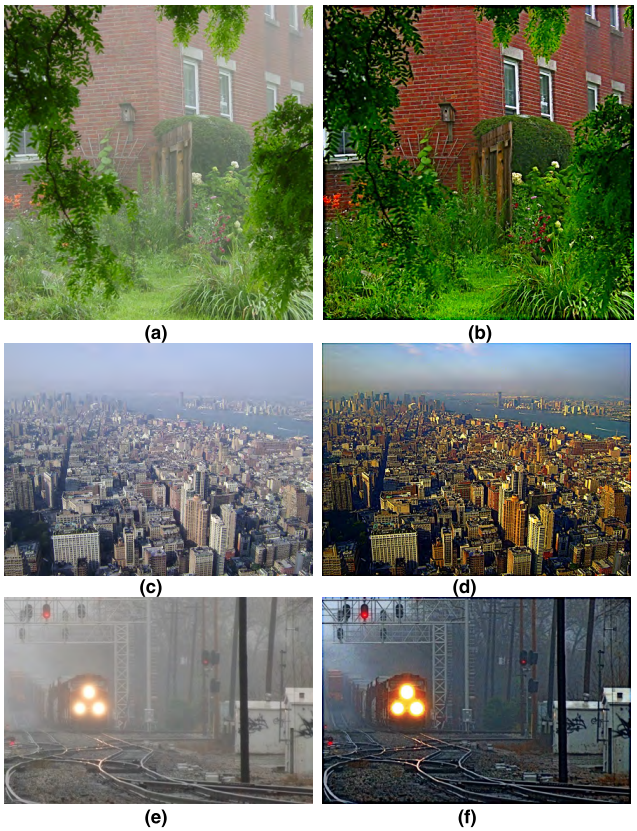

FIGURE 7. (a)(c)(e) Input foggy images, (b)(d)(f) Reconstructed images respectively.

IV. EXPERIMENTAL RESULTS

Experiments are performed on a variety of images and the results are compared with five state-of-the-art existing image defogging algorithms, i.e., Tan [3], He *et al.* [4], Caraffa and Tarel [29], Fattal [30], and Wang and Fan [31]. We performed quantitative and qualitative analysis on two

types of images which include images with smooth depth and the other with cluttered depth [31]. Images with bright objects such as buildings, clouds, cars and small sky region may cause wrong estimation of atmospheric light and may lead to wrong estimation of depth. Such images are classified as smooth depth image category. In contrast, images with small foreground objects such as leaves and decoration pieces introduce discontinuities in foreground objects that produces complex depth. Therefore, such images are categorized as cluttered depth images. Different authors used different parameters to evaluate their results, some common parameters are SSIM and FE. Structural similarity (SSIM), fog effect (FE), degradation score (DS) and anisotropic quality index (AQI) are calculated to compare our results with other image defogging algorithms.

$$FogEffect = 10 \cdot \log_{10}\left(\frac{MAX^2}{MSE}\right) \tag{17}$$

where MAX represents maximum possible value of input image and MSE is Mean Square Error. It is given as,

$$MSE = \frac{1}{mn}\sum_{i=0}^{m-1}\sum_{j=0}^{n-1}[I\,(i,j) - K\,(i,j)]^2 \tag{18}$$

where I is input foggy image, K is fog free reconstructed image, $m \times n$ is size of the image [32].

$$SSIM\,(x,y) = \frac{\left(2\mu_x\mu_y + c_1\right)\left(2\sigma_{xy} + c_2\right)}{\left(\mu_x^2 + \mu_y^2 + c_1\right)\left(\sigma_x^2 + \sigma_y^2 + c_2\right)} \tag{19}$$

where x and y are two windows of common size, μ_x, and μ_y are mean of windows while σ_x^2 and σ_y^2 are their variances, σ_{xy} is covariance, c_1 and c_2 are constants. A reference image is required to calculate SSIM and Fog Effect, as there is no ground truth image available for these foggy images therefore we used foggy image as reference image to calculate Fog Effect and SSIM as in [31]. Lower value of SSIM and Fog Effect implies that reconstructed image is different from foggy image with a greater margin. We would like to elaborate that, SSIM and FE only show that reconstructed image is different from foggy image, but it does not mean that if an image is different from foggy image then it should be the finest image. These parameters have been mostly used by Riaz *et al.* [8], He *et al.* [18], and Wang and Fan [31] to evaluate their performance therefore a comparison was necessary with the proposed algorithm. AQI is a non-reference state-of-the-art method to compute image quality. Unlike other measures no reference image is required to compute AQI. Higher the value of AQI means better the quality of image. The model used to assess the degradation score has an output ranging from 0 to 100. The value of 0 signifies a pristine image and a value of 100 signifies a most distorted image. There are some other parameters, such as, sharpness, contrast and naturalness, which may also be used for the evaluation of defogging algorithms. El Khoury *et al.* [33] proposed a metric to evaluate the colors of an image, and Gu *et al.* [34] proposed a non-reference parameter for the evaluation of sharpness. Two other non-reference parameters are also used in literature including Image Quality Assessment (IQA) [35] for the evaluation of color contrast based on information maximization, and Blind Image Quality Assessment (BIQA) [36] using brain theory based on free energy to evaluate image naturalness. Min *et al.* also proposed two different algorithms to calculate BIQA [37] and Blind Quality Assessment (BQA) [38]. BIQA is based on distortion aggravation levels and BQA is based on Pseudo Reference Image (PRI).

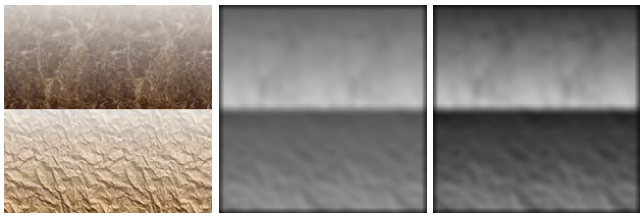

FIGURE 8. (a) Synthetic foggy image, (b) Refined transmission map by (13), (c) Refined transmission map by (12).

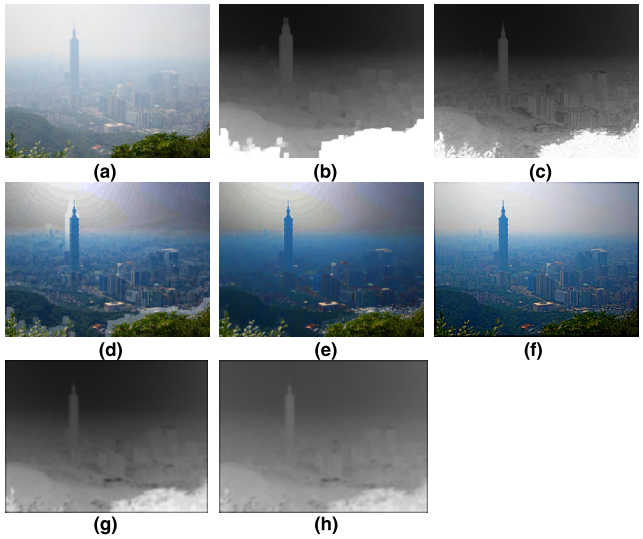

FIGURE 9. (a) Input foggy image (b) Transmission map calculated by DCP with patch 19 (c) Transmission map calculated by Wang's method [31] (d) Reconstructed image by DCP (e) Reconstructed image by Wang's method (f) Reconstructed image by proposed method (g) Transmission map calculated by proposed method (12) (h) Transmission map calculated by proposed method (13).

A. EDGE-PRESERVED DEPTH FUSION

The transmission map is refined with edge preservation which results in better reconstruction of fog free image. Fig.8 shows edge preserved refined transmission map of two albedos synthetic images. Transmission map calculated by DCP using patch size 19 is shown in Fig.9 (b). Transmission maps calculated by Wang's method is shown in Fig.9 (c) and two transmission maps calculated by proposed method are shown in Fig.9 (g) and (h). Images defogged by state-of-the-art methods and proposed method are shown in Fig.9 (d), (e) and (f). Foggy image of Taipei downtown is an example of smooth depth. Wang and Fan [31] observed halo

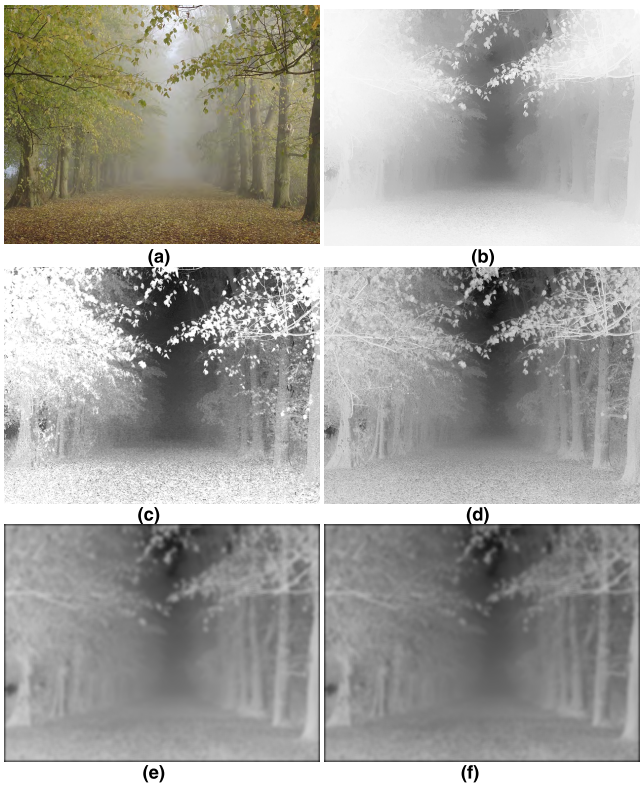

FIGURE 10. (a) Input foggy image (b) Transmission map calculated by He's method, (c) Transmission map calculated by Fattal's method, (d) Transmission map calculated by Wang's method (e) Transmission map calculated by proposed method (13), (f) Transmission map calculated by proposed method (12).

effects in image reconstructed by DCP based method as seen in Fig. 9 (d) and tried to remove these effects, but a few halo effects can still be seen in sky area of image reconstructed by his method as shown in Fig. 9 (e). Halo effects were also present in image reconstructed by Tan [3] and He *et al.* [4]. The image reconstructed by proposed method is shown in Fig.9 (f). It can be seen that the proposed method removes the halo effects.

Fig.10 (a) with leaves in foreground is an example of cluttered-depth. Fig.10 (b) shows transmission map calculated by He's method, Fig.10 (c) is the outcome by Fattal's method while Fig.10 (d) shows the result by Wang's method. Fig.10 (e-f) shows transmission maps calculated by proposed method. It can be seen that the transmission maps of the proposed method show more detail information as compared to other methods.

Fig.11 (a) is also an example of cluttered depth because of the leaves in the foreground. Fig.11 (b) shows the transmission map refined by guided filter and Fig.11 (c) shows corresponding reconstructed image. Fig.11 (d) and Fig.11 (e) show the transmission maps refined by proposed method and Fig.11 (f) shows the corresponding image reconstructions. It can be observed that the proposed method accurately estimates depth information from smooth depth as well as cluttered depth images and generates defogged images visually more appealing as compared to other methods.

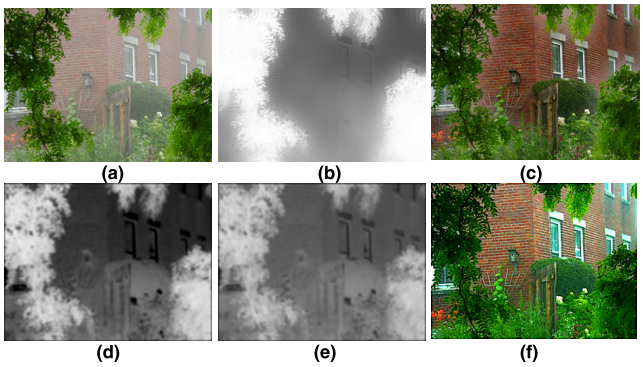

FIGURE 11. (a) Input foggy image (b) Transmission map refined by guided filter (c) Image reconstructed by using (b), (d) Refined transmission map calculated by proposed method (13), (e) Refined transmission map calculated by proposed method (12) (f) Reconstructed image by proposed method.

B. DEFOGGING ALGORITHM ANALYSIS

Images reconstructed by proposed methodology are compared with the images reconstructed by existing image defogging methods. Structural similarity (SSIM), fog effect (FE), anisotropic quality index (AQI), and degradation score (DS) are computed to compare results for smooth and clutter depth images.

Example of a smooth depth image is covered in Fig.12 and Fig.13, which show images defogged by several state-of-the-art algorithms and the proposed. Similarly, case of clutter depth image is shown in Fig.14 which also provides a promising comparison of several different algorithms and the proposed approach. In all the images our methodology outperforms existing image defogging techniques to produce favorable outcome.

Performance measurement for these images in terms of SSIM, FE, AQI and DS are shown in Table 1. The proposed method computes images with lowest SSIM and lowest Fog Effect indicating that the defogged images obtained through the proposed method are different from the reference foggy images with greater margin. While the highest value of AQI and lowest value of DS indicates that proposed method has reconstructed image with improved quality and less degradation.

Fig.12 (a) is an example of smooth depth image. Since the image is a long distance capture, small sky region is also visible and no foreground object is present in the scene hence it is classified as smooth depth image. Fig.12 (b)-(g) show defogged images obtained by different methods including ours. Image defogged by Fattal's i.e., Fig.12 (b) has a washed out effect. Fig.12 (c) is defogged image result by He's method and is generally blurred and objects that are farther appear darker. Tan's method in Fig.12 (d) appears to have poor color contrast. Similarly, Tarel's method in Fig. 12 (e) and Wang's approach in Fig. 12 (f) appear with clustered and degraded contrast respectively. In contrast, image defogged by the proposed method as shown in Fig.12 (g) is sharp where objects near and farther away from camera are equally defogged.

TABLE 1. Performance evaluation.

Technique	Figure 12				Figure 13				Figure 14			
	SSIM	FE	AQI	DS	SSIM	FE	AQI	DS	SSIM	FE	AQI	DS
Fattal	0.8686	16.1377	0.0019	4.166	0.8802	17.1154	0.0057	14.28	0.8184	18.9387	0.0006	20.0
He	0.8514	14.6418	0.0011	7.5	0.7642	13.1732	0.0048	14.28	0.7523	12.1402	0.0004	24.54
Tan	0.6515	11.7306	0.0026	10.41	0.6463	12.143	0.0087	20.71	0.4636	9.0192	0.0011	32.72
Tarel	0.9119	17.8932	0.0005	17.29	0.818	17.3694	0.0047	20.0	0.7516	12.4087	0.0001	39.09
Wang	0.6893	12.4586	0.0020	12.5	0.7346	13.2091	0.0043	27.14	0.5548	9.1805	0.0017	29.09
Proposed	0.6265	11.5254	0.0028	2.5	0.5738	10.6752	0.0159	11.42	0.6218	10.4135	0.0018	16.36

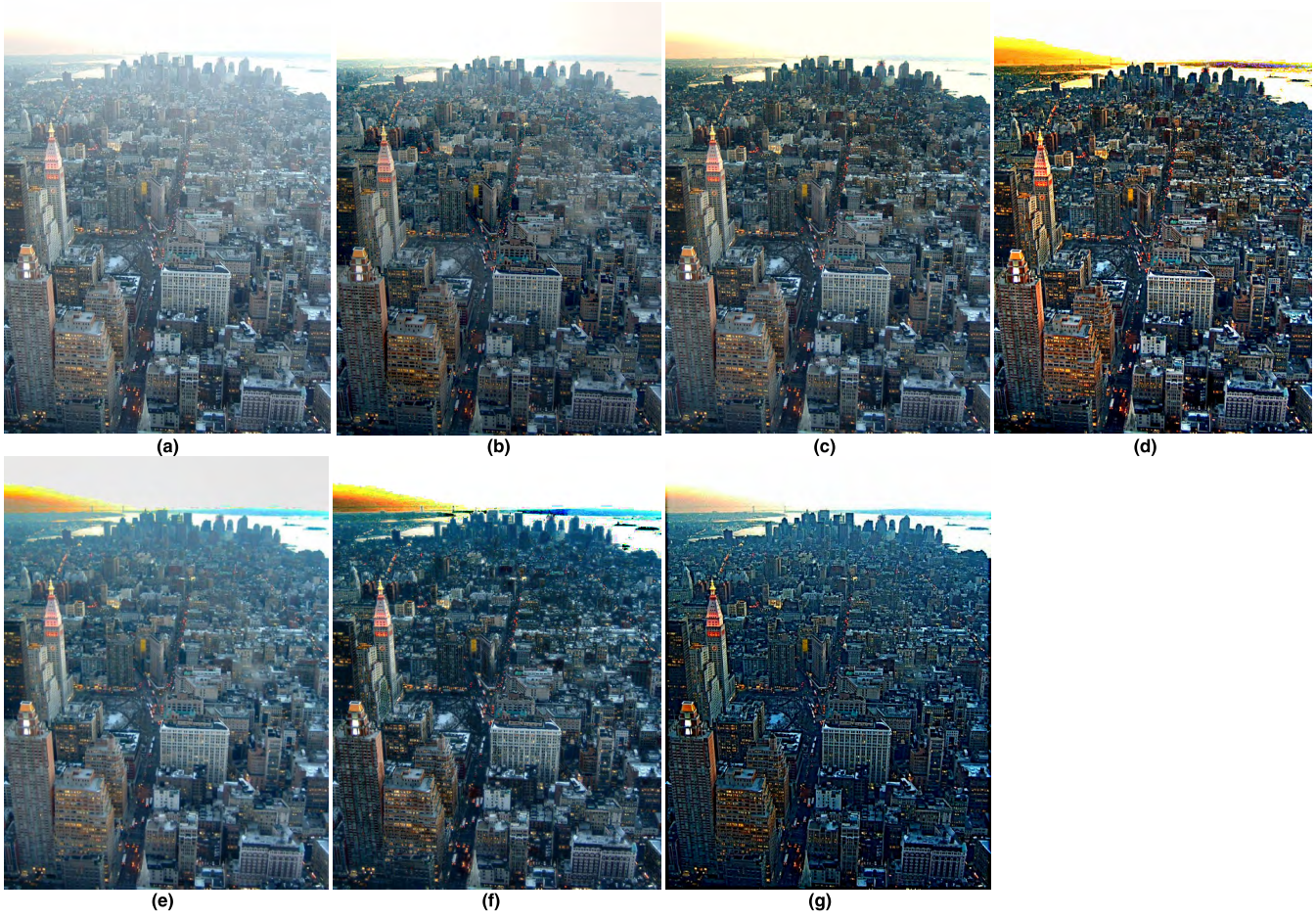

FIGURE 12. (a) Input foggy image, reconstructed image by (b) Fattal (c) He (d) Tan (e) Tarel (f) Wang and (g) Proposed method.

Fig.13 (a) is classified as smooth depth, due to presence of, white clouds and white stones on mountain and absence of foreground objects together with suddenly changing intensities. Image defogged by Fattal's method is shown in Fig.13 (b) in which fog is still present. Fig.13 (c) shows image defogged by He's method which is blurred and clouds in sky are completely white. Fig.13 (d) shows image defogged by Tan's method where circular artifacts are seen in sky region. Image defogged by Tarel's method is shown in Fig.13 (e), once again artifacts and fog can be seen in their defogged image. Fig.13 (f) shows image defogged by Wang's method has some artifacts on edge of mountain. Fig.13 (g) is image defogged by proposed method. It can be seen that image contrast is improved, sky region of image is also good in contrast with no artifacts.

Fig.14 (a) is categorized as clutter depth image, because we can see trees, branches and stems that have high frequency detail information. Fig.14 (b) shows image defogged by Fattal's method which is bad in contrast. Similarly, image defogged by He's method in Fig.14 (c) appears hazy although

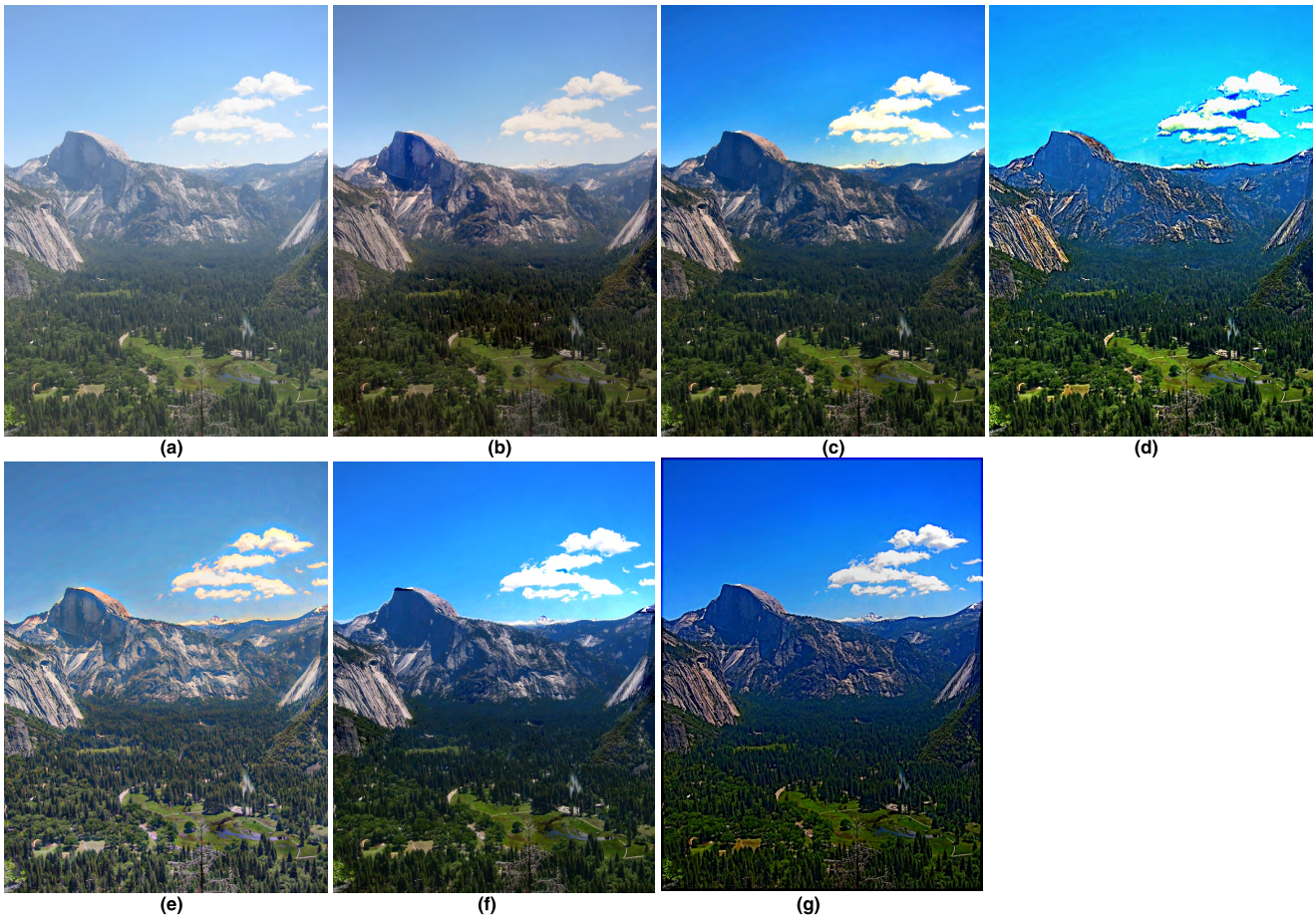

FIGURE 13. (a) Input foggy image, reconstructed image by (b) Fattal (c) He (d) Tan (e) Tarel (f) Wang and (g) Proposed method.

FIGURE 14. (a) Input foggy image, reconstructed image by (b) Fattal (c) He (d) Tan (e) Tarel (f) Wang and (g) Proposed method.

fog factor is removed to some extent. The result acquired through Tan's, Tarel's and Wang's method are also not successful in removing fog completely. Here, our method again out-performs the rest to produce visually appealing images.

Although image defogging itself is a challenging task, but for images which covers a large sky area, it becomes even more challenging task to defog them due to presence of sun or clouds. Block artifacts becomes more prominent in

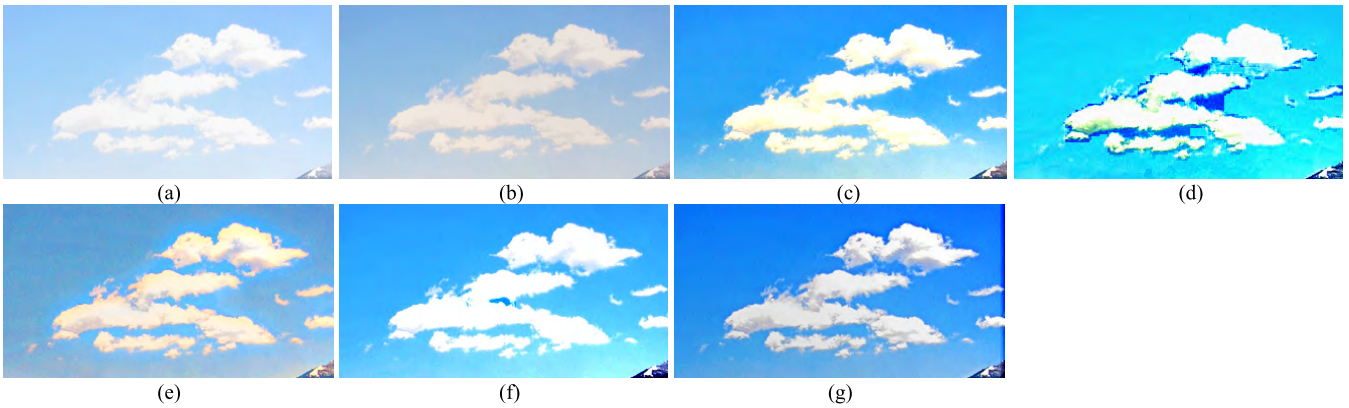

FIGURE 15. (a) Input foggy image, reconstructed image by (b) Fattal (c) He (d) Tan (e) Tarel (f) Wang and (g) Proposed method.

sky regions. As already discussed in section 1 [9], [10] different algorithms are proposed to calculate transmission map for sky regions and non-sky regions.

Clouds are present in images with sky region as shown in Fig. 13. The zoomed in version of these images are shown in Fig. 15. Clouds and the area surrounding the clouds is best reconstructed by the proposed method as compared to previously proposed methods as shown in Fig. 15 (g). Images shown in Fig.15 (b)-(f) are reconstructed by previously proposed method.

V. CONCLUSION

In this work, image defogging method has been proposed based on the dark channel prior (DCP). Existing state-of-the-art image defogging methods using DCP fail to show optimal performance for the task of image defogging. Their results are either low in contrast or compromised by artifacts. We have proposed a new method to calculate the transmission map and utilized a Laplacian filter to refine the transmission map. Experimental results show that the proposed method estimates fog more accurately and the reconstructed images have better color contrast. Halo effects and thin fog layer which can be seen in defogged images of other methods are removed using the proposed method. Furthermore, Fog Effect, SSIM, DS and AQI values show that the images reconstructed by proposed method exhibit higher perceptual quality as compared to existing image defogging methods. In future our proposed method can be improved to reconstruct fog free image from dense foggy image also algorithm can be optimized to reconstruct fog free image on run time.

REFERENCES

[1] X. He J. Mao, Z. Liu, J. Zhou, and Y. Hua, "A fast algorithm for image defogging," in *Proc. Chin. Conf. Pattern Recognit.* Berlin, Germany: Springer-Verlag, 2014, pp. 149–158.

[2] Z. Chen, J. Shen, and P. Roth, "Single image defogging algorithm based on dark channel priority," *J. Multimedia*, vol. 8, no. 4, pp. 432–438, 2013.

[3] R. T. Tan, "Visibility in bad weather from a single image," in *Proc. IEEE Conf. Comput. Vis. Pattern Recognit.*, Jun. 2008, pp. 1–8.

[4] K. He, J. Sun, and X. Tang, "Single image haze removal using dark channel prior," *IEEE Trans. Pattern Anal. Mach. Intell.*, vol. 33, no. 12, pp. 2341–2353, Dec. 2011.

[5] A. Kumari, S. Sahdev, and S. K. Sahoo, "Improved single image and video dehazing using morphological operation," in *Proc. IEEE Int. Conf. VLSI Syst., Architecture, Technol. Appl.*, Jan. 2015, pp. 1–5.

[6] N. Baig, M. M. Riaz, A. Ghafoor, and A. M. Siddiqui, "Image dehazing using quadtree decomposition and entropy-based contextual regularization," *IEEE Signal Process. Lett.*, vol. 23, no. 6, pp. 853–857, Jun. 2016.

[7] G. Meng, Y. Wang, J. Duan, S. Xiang, and C. Pan, "Efficient image dehazing with boundary constraint and contextual regularization," in *Proc. IEEE Int. Conf. Comput. Vis.*, Dec. 2013, pp. 617–624.

[8] I. Riaz, T. Yu, Y. Rehman, and H. Shin, "Single image dehazing via reliability guided fusion," *J. Vis. Commun. Image Represent.*, vol. 40, pp. 85–97, Oct. 2016.

[9] E. Zhang, K. Lv, Y. Li, and J. Duan, "A fast video image defogging algorithm based on dark channel prior," in *Proc. 6th Int. Congr. Image Signal Process. (CISP)*, vol. 1, 2013, pp. 219–223.

[10] H. Xu, J. Guo, Q. Liu, and L. Ye, "Fast image dehazing using improved dark channel prior," in *Proc. IEEE Int. Conf. Inf. Sci. Technol.*, Mar. 2012, pp. 663–667.

[11] L. Deng, O. Li, and S. Zhao, "An improved image defogging algorithm based on global dark channel prior and fuzzy logic control," in *Proc. IEEE Wavelet Active Media Technol. Inf. Process.*, Dec. 2015, pp. 188–191.

[12] X. Chen and W. Sun, "A fast algorithm for single image dehazing based on estimating illumination veil," in *Proc. Int. Conf. Mechatronics, Electron., Ind. Control Eng.*, 2015, pp. 987–991.

[13] B. Yao, L. Huang, and C. Liu, "Adaptive defogging of a single image," in *Proc. IEEE Int. Symp. Comput. Intell. Design*, vol. 1, Dec. 2009, pp. 56–59.

[14] M. J. Abbaspour, M. Yazdi, and M. M. Shirazi, "A new fast method for foggy image enhancement," in *Proc. Iranian Conf. Elect. Eng. (ICEE)*, 2016, pp. 1855–1859.

[15] J. P. Tarel and N. Hautiere, "Fast visibility restoration from a single color or gray level image," in *Proc. IEEE 12th Int. Conf. Comput. Vis.*, Sep./Oct. 2009, pp. 2201–2208.

[16] I. Yoon, J. Jeon, J. Lee, and J. Paik, "Weighted image defogging method using statistical RGB channel feature extraction," in *Proc. SoC Design Conf.*, 2010, pp. 34–35.

[17] I. Yoon, J. Jeon, J. Lee, and J. Paik, "Spatially adaptive image defogging using edge analysis and gradient-based tone mapping," in *Proc. IEEE Int. Conf. Consum. Electron.*, Jan. 2011, pp. 195–196.

[18] L. He, J. Zhao, N. Zheng, and D. Bi, "Haze removal using the difference-structure-preservation prior," *IEEE Trans. Image Process.*, vol. 26, no. 3, pp. 1063–1075, Mar. 2017.

[19] S. Lee, S. Yun, J. H. Nam, C. S. Won, and S. W. Jung, "A review on dark channel prior based image dehazing algorithms," *EURASIP J. Image Video Process.*, vol. 2016, no. 1, p. 4, 2016.

[20] J. Tang, "Single image defogging based on step estimation of transmissivity," in *Proc. Chin. Conf. Image Graph. Technol.* Singapore: Springer, 2018.

[21] M. I. Anwar and A. Khosla, "Vision enhancement through single image fog removal," *Eng. Sci. Technol., Int. J.*, vol. 20, no. 3, pp. 1075–1083, 2017.

[22] N. S. Pal, S. Lal, and K. Shinghal, "Visibility enhancement of images degraded by hazy weather conditions using modified non-local approach," *Optik*, vol. 163, pp. 99–113, Jun. 2018.
[23] A. Li and X. Li, "A novel image defogging algorithm based on improved bilateral filtering," in *Proc. 10th Int. Symp. Comput. Intell. Design (ISCID)*, vol. 2, 2017, pp. 326–331.
[24] M. Zhu, B. He, and Q. Wu, "Single image dehazing based on dark channel prior and energy minimization," *IEEE Signal Process. Lett.*, vol. 25, no. 2, pp. 174–178, Feb. 2018.
[25] C. Chengtao, Z. Qiuyu, and L. Yanhua, "Improved dark channel prior dehazing approach using adaptive factor," in *Proc. IEEE Int. Conf. Mechatronics Autom. (ICMA)*, Aug. 2015, pp. 1703–1707.
[26] J. Jackson, "Hybrid single image dehazing with bright channel and dark channel priors," in *Proc. IEEE 2nd Int. Conf. Image, Vis. Comput. (ICIVC)*, Jun. 2017, pp. 381–385.
[27] Z. Li and J. Zheng, "Single image de-hazing using globally guided image filtering," *IEEE Trans. Image Process.*, vol. 27, no. 1, pp. 442–450, Jan. 2018.
[28] D. Nair and P. Sankaran, "Color image dehazing using surround filter and dark channel prior," *J. Vis. Commun. Image Represent.*, vol. 50, pp. 9–15, Jan. 2018.
[29] L. Caraffa and J. P. Tarel, "Markov random field model for single image defogging," in *Proc. IEEE Intell. Veh. Symp.*, Jun. 2013, pp. 994–999.
[30] R. Fattal, "Single image dehazing," *ACM Trans. Graph.*, vol. 27, no. 3, pp. 60–72, 2008.
[31] Y. Wang and C. Fan, "Single image defogging by multiscale depth fusion," *IEEE Trans. Image Process.*, vol. 23, no. 11, pp. 4826–4837, Nov. 2014.
[32] Z. Wang and A. C. Bovik, "Mean squared error: Love it or leave it? A new look at signal fidelity measures," *IEEE Signal Process. Mag.*, vol. 26, no. 1, pp. 98–117, Jan. 2009.
[33] J. El Khoury, Jessica, S. Le Moan, J.-B. Thomas and A. Mansouri, "Color and sharpness assessment of single image dehazing," *Multimedia Tools Appl.*, pp. 1–22, Sep. 2017, doi: 10.1007/s11042-017-5122-y.
[34] K. Gu, G. Zhai, W. Lin, X. Yang, and W. Zhang, "No-reference image sharpness assessment in autoregressive parameter space," *IEEE Trans. Image Process.*, vol. 24, no. 10, pp. 3218–3231, Oct. 2015.
[35] K. Gu, W. Lin, G. Zhai, X. Yang, W. Zhang, and C. W. Chen, "No-reference quality metric of contrast-distorted images based on information maximization," *IEEE Trans. Cybern.*, vol. 47, no. 12, pp. 4559–4565, Dec. 2017.
[36] K. Gu, G. Zhai, X. Yang, and W. Zhang, "Using free energy principle for blind image quality assessment," *IEEE Trans. Multimedia*, vol. 17, no. 1, pp. 50–63, Jan. 2015.
[37] X. Min, G. Zhai, K. Gu, Y. Liu, and X. Yang, "Blind image quality estimation via distortion aggravation," *IEEE Trans. Broadcast.*, vol. 64, no. 2, pp. 508–517, 2018.
[38] X. Min, K. Gu, G. Zhai, J. Liu, X. Yang, and C. W. Chen, "Blind quality assessment based on pseudo reference image," *IEEE Trans. Multimedia*, to be published, doi: 10.1109/TMM.2017.2788206.

ZAHID TUFAIL received the B.S. degree in electrical engineering from the University of Engineering and Technology, Lahore, Pakistan, in 2014. He is currently pursuing the M.S. degree in electrical engineering with the Institute of Space Technology, Islamabad, Pakistan.

KHAWAR KHURSHID received the Ph.D. degree in biomedical imaging systems from Michigan State University. He is currently heading the Institute of Applied Electronics and Computers, National University of Sciences and Technology, Pakistan. He is the Director of the Center of Excellence in FPGA and ASIC Research. He specializes in medical imaging, embedded systems, pattern recognition, image and signal processing with research interests in the areas of wearable devices, image segmentation, registration, video encoding, multimedia streaming, and 3-D display systems.

AHMAD SALMAN received the master's degree in electrical engineering from the National University of Sciences and Technology (NUST), Islamabad, Pakistan, and the Ph.D. degree from The University of Manchester, U.K., with specialization in machine learning and signal processing. He is currently an Assistant Professor with the School of Electrical Engineering and Computer Science, NUST. He is leading the Optimization and Machine Learning Research Group.

IMRAN FAREED NIZAMI received the B.Sc. degree (Hons.) in computer engineering from the University of Engineering Technology Taxila, Pakistan, and the M.S. degree in electrical and electronic engineering from Yonsei University, South Korea. He is currently pursuing the Ph.D. degree with National University of Sciences and Technology, Pakistan. His research interests include, computational intelligence, pattern recognition, and signal processing.

KHURRAM KHURSHID received the B.E. degree (Hons.) in software engineering from the National University of Sciences and Technology, Islamabad, in 2002, and the Ph.D. degree from Paris Descartes University, France, in 2009. He has been associated with the Institute of Space Technology (IST), Pakistan, since 2002. He is currently heading the Electrical Engineering Department and looking after the Signal and Image Processing Research Group. He has been involved in different research ventures in the field of image processing, pattern recognition, and computer vision. He is one of the founding members of the Pakistan Pattern Recognition Society. He is also the Project Manager of the Small Satellite CubeSat Program of IST and ICUBE. The first cubeSat satellite of this project (ICUBE-1) was successfully launched in 2013.

BYEUNGWOO JEON (SM'97) received the B.S. and M.S. degrees from the Department of Electronics Engineering, Seoul National University, Seoul, South Korea, in 1985 and 1987, respectively, and the Ph.D. degree from the School of Electrical Engineering, Purdue University, USA, in 1992. From 1993 to 1997, he was with the Signal Processing Lab, Samsung Electronics, South Korea, where he conducted research and development into video compression algorithms, design of digital broadcasting satellite receivers, and other MPEG-related research for multimedia applications. Since 1997, he has been with the Faculty of the School of Information and Communication Engineering, Sungkyunkwan University, South Korea, where he is currently a Professor. He was a Visiting Scientist at MIT, USA, from 2006 to 2007, and the Institute for Infocomm Research, Singapore, in 2010. He served as a Project Manager of Digital TV and Broadcasting in the Korean Ministry of Information and Communications from 2004 to 2006, where he supervised all digital TV-related research and development in South Korea. His research interests include multimedia signal processing, video compression, statistical pattern recognition, and remote sensing. He is member of SPIE, IEEK, KICS, and KSOBE.